ORIGINAL RESEARCH PAPER

Chemistry

KEY WORDS: Fluoropyrazine species, vibrational spectra, molecular structure, descriptor properties, DFT calculations

EFFECT OF CARBOXYL AND CARBOXAMIDE SUBSTITUENT GROUPS ON FLUORINATED PYRAZINE SPECIES WITH ANTITUBERCULAR ACTIVITIES

Maximiliano A. Iramain Cátedra de Química General, Instituto de Química Inorgánica, Facultad de Bioquímica. Química y Farmacia, Universidad Nacional de Tucumán, Ayacucho 471, (4000) San Miguel de Tucumán, Tucumán, Argentina

Silvia Antonia Brandán Cátedra de Química General, Instituto de Química Inorgánica, Facultad de Bioquímica. Química y Farmacia, Universidad Nacional de Tucumán, Ayacucho 471, (4000) San Miguel de Tucumán, Tucumán, Argentina

ABSTRACT

The structural, electronic, topological and vibrational properties were studied for F-pyrazine, 3-fluoropyrazine-2-carboxilic acid and 3-fluoropyrazine-2-carboxamide in gas phase by using the hybrid B3LYP/6-311++G** level of theory. Theoretically, two conformations were found for both acid and amide species being their C2 conformations, with C_s symmetries, the most stable. The NBO study reveals the high stability of the acid species due to the two ΔET_{LP^*} and ΔET_{LPLP^*} interactions not observed in the amide species. The AIM analysis supports the high stabilities of both C2 conformers due to the halogen bonds formation where the topological properties are higher for the acid species, in very good concordance with the higher total energy observed by NBO calculations. The frontier orbitals predict a higher reactivity for the amide species while the descriptors evidence the higher nucleophilicity and electrophilicity indexes for the acid species. On the other hand, the C2-N3 stretching mode in FP is predicted at higher wavenumbers than pyrazine while in the acid and amide species this stretching mode is predicted with partial double bond at lower wavenumbers. The tentative assignments for the acid and amide species were performed. The force constants calculated show strongly dependence from their geometrical parameters.

INTRODUCTION

New fluorinated pyrazine carboxamide compounds have been synthesized as anti-turbeculars agents as a consequence of the strong resistance developed by the microorganism that cause the infectious tuberculosis (TB) disease, *Mycobacterium tuberculosis* [1-8]. The F atom is the better halogen substituent to be incorporated to the pyrazine structure due to their smallest size and strongest electronegativity [1] while due to their biological properties pyrazine carboxamide is an important component in the intensive phase of short-course treatment of TB, as reported by Ugwu et al. [2]. For these reasons, the knowledge of all properties related to these compounds is of great chemical, biological, pharmacological and medicinal interest to prepare novel drugs with better properties. Hence, the interest to study the structural, electronic, topological and vibrational properties of 3-fluoropyrazine-2-carboxilic acid and 3-fluoropyrazine-2-carboxamide compounds by using hybrid calculations derived from the density functional theory (DFT). So far, the structure of these two substances were not reported and only for pyrazine [9] pyrazincarboxanamide structures [10,11], carboxylic acids [12] and their electronic properties were already published [13]. In relation a their infrared and Raman spectra they were not reported for 3-fluoropyrazine-2-carboxilic acid and 3-fluoropyrazine-2-carboxamide and only the infrared and Raman spectra of some pyrazine [14-16], 2,6-dichloropyrazine [17] and N-[(4-(trifluoromethyl) phenyl]pyrazine-2-carboxamide were studied [18]. Hence, in order to identify these species by using the vibrational spectroscopy in different media are of great interest and useful to analyze those spectra. In this context, the aims of this work are to: (i) evaluate the change in the structural, electronic, topological and vibrational properties when the carboxyl and carboxamide groups are incorporated as substituent to fluorinated pyrazine species, (ii) predict the infrared and Raman spectra of the two fluorinated pyrazine species, (iii) perform the complete vibrational assignments of these species and, finally (iv) compare their main force constants. To those purposes their atomic charges, molecular electrostatic potential, bond orders, stabilization energies and topological properties were studied for those species in gas phase by using the hybrid B3LYP/6-311++G** level of theory and NBO, AIM, bond orders, molecular electrostatic potentials and frontier orbitals calculations [19-24]. Useful descriptors were used to predict the behaviours of these species [25-27] while the harmonic force fields and force constants were calculated with the SQMFF procedure and the Molvib program [28,29]. Then, those properties were deeply analyzed and compared among them to find, first, the effect that generate on the properties when the F atom is incorporate in the pyrazine ring and, later to analyze the consequence of include the carboxyl and carboxamide substituents on the F-pyrazine species. Esfahanizadeh et al. [1] have reported for the acid and amide compounds the minimum bactericidal concentration > 12.5 MIC µg/mL but these values are strongly dependent from the pH.

COMPUTATIONAL DETAILS

The pyrazine (P), F-pyrazine (FP), 3-fluoropyrazine-2-carboxilic acid (FPCOOH) and 3-fluoropyrazine-2-carboxamide ($FPCONH_2$) structures were modelled with the *GaussView* program [27] and optimized by using the Gaussian 09 program [28] with the hybrid B3LYP/6-311++G** method. Here, P was optimized with both C_s and D_{2h} symmetries while two stable structures were found on the potential energy surface for $FPCONH_2$ and FPCOOH named C1 and C2, both with C_1 symmetries. The theoretical structures of all these species are presented in Figure 1. The volumes in gas phase were calculated at the same level of theory with the Moldraw program [32]. The properties, such as atomic natural population (NPA) and the Merz-Kollman (MK) charges, the molecular electrostatic potential (MEP), bond orders, expressed as Wiberg indexes, stabilization energies and topological properties were studied for those species [19,22]. The topological parameters were computed with the AIM2000 program [20,21] while the SQMFF methodology [28] and the Molvib program [29] were used together with the corresponding internal coordinates to calculate the force fields for all the species. The complete vibrational assignments and the Raman spectra were predicted for the most stable structures of 3-fluoropyrazine-2-carboxilic acid (FPCOOH) and 3-fluoropyrazine-2-carboxamide ($FPCONH_2$) by using the Potential Energy Distribution (PED) contributions 10%. The harmonic force fields were transformed from cartesian coordinates to normal internal coordinates in order to obtain the force constants. The frontier orbitals [23,24] together with well-known descriptors were calculated in order to predict the reactivities and behaviours of all species and to know why those compound present interesting biological properties [25-27].

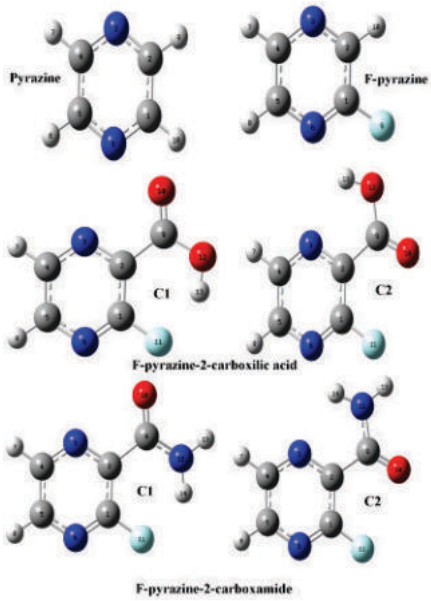

Figure 1. Theoretical structures of pyrazine, F-pyrazine, 3-fluoropyrazine-2-carboxilic acid and 3-fluoropyrazine-2-carboxamide in gas phase by using the hybrid B3LYP/6-311++G** level of theory.

RESULTS AND DISCUSSION

OPTIMIZATIONS IN GAS PHASE

The calculated total energies, dipole moments and volume variation for the two optimized P structures, FP and, the two C1 and C2 conformers of FPCOOH and $FPCONH_2$ can be seen in **Table 1** while in **Figure 2** are represented the modifications observed on these properties when the F atom is incorporated to pyrazine ring and, then when the COOH and $CONH_2$ groups are incorporated to fluoropyrazine. Obviously, the energies values increase with the group, as expected because increase the numbers of atoms while, for both pyrazine species the energies are the same independently of the symmetry. In relation to the dipole moment values the carboxylic species present the higher value, being C2 the most voluminous species of FPCOOH while for $FPCONH_2$ the higher volume is observed for C1. Note that both most stable C2 conformations of FPCOOH and $FPCONH_2$ have the higher dipole moment values, as also was observed in other species [33-37]. This way, such observations could probably be related to the higher stabilities of the species as a consequence of their higher dipole moments. On the other side, pyrazine has dipole moment null and when the F atom is incorporate to the ring structure clearly increases the dipole moment of pyrazine to 1.70 D. **Figure 3** shows the orientations and magnitudes of the vectors corresponding to the dipole moments of FP, FPCOOH and $FPCONH_2$ species where we can easily observe the change in size and direction, especially when the group change from FP to FPCOOH and from FPCOOH to $FPCONH_2$. The higher dipole moment value observed for the carboxylic acid species can be explained because the electronegativity of OH group is between 3.51 [38] and 2.68 [39] where for the carboxy group it is reported values between 3.49 [38] and 2.8 [39] while the amino group present lower values, which are between 2.61 [38] and 2.42 [39]. These results show clear structural differences between the acid and amide species being the C2 conformer of FPCOOH most polar and voluminous. When the populations are analyzed from Table 1 we observed that the energies differences existent between both conformers of FPCOOH and $FPCONH_2$ are high and, as a consequence only the C2 conformers are expected in both species.

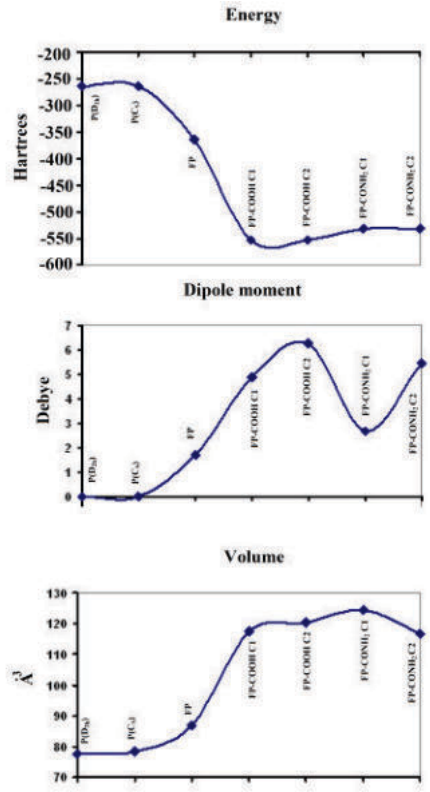

Figure 2. Calculated total energies, dipole moments and volume variation for the pyrazine, F-pyrazine, 3-fluoropyrazine-2-carboxilic acid and 3-fluoropyrazine-2-carboxamide structures in gas phase by using the hybrid B3LYP/6-311++G** level of theory.

TABLE – 1

Calculated total energies (E), dipole moments (μ), volume and populations for pyrazine (P), F-pyrazine (FP), 3-fluoropyrazine-2-carboxilic acid (FPCOOH) and 3-fluoropyrazine-2-carboxamide ($FPCONH_2$) in gas phase.

B3LYP/6-311++G** method					
Species	E (Hartrees)	E (kJ/mol)	μ (D)	V (□³)	Pop %
P (D_{2h})	-264.3873	0.00	0.0	77.7	100
P (C_s)	-264.3873		0.0	78.4	
FP	-363.3611	0.00	1.70	86.8	100
Acid C1	-552.2794	22.58	4.87	117.5	0.0
Acid C2	-552.2880	0.00	6.25	120.2	100
Amide C1	-532.4131	14.43	2.69	124.6	0.3
Amide C2	-532.4186	0.00	5.44	116.7	99.7

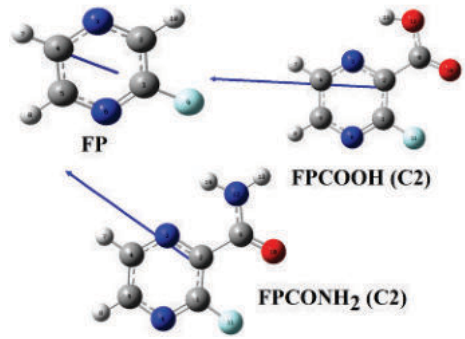

Figure 3. Orientations and magnitudes of the vectors corresponding to the dipole moments of FP, FPCOOH and $FPCONH_2$ species in gas phase by using the hybrid B3LYP/6-311++G** level of theory.

TABLE – 2

Comparison of calculated geometrical parameters for pyrazine (P), F-pyrazine (FP), 3-fluoropyrazine-2-carboxilic acid (FPCOOH) and 3-fluoropyrazine-2-carboxamide ($FPCONH_2$) in gas phase compared with the corresponding experimental ones for two forms of Pyrazincarboxamide.

Parameters	B3LYP/6-311++G**[a]						Pyrazincarboxamide	
	Pyrazine	F-pyrazine	F-pyrazine-2-carboxil acid		F-pyrazine-2-carboxamide		β form	δ form
			C1	C2	C1	C2	Exp[b]	Exp[c]
			Bond lengths (Å)					
C1-F11	1.085	1.342	1.358	1.324	1.354	1.326		
C1-N6	1.334	1.307	1.303	1.311	1.305	1.312	1.335	1.329
C5-N6	1.334	1.339	1.334	1.334	1.335	1.334	1.333	1.337
C2-N3	1.334	1.328	1.333	1.334	1.333	1.335	1.334	1.352
C4-N3	1.335	1.338	1.329	1.331	1.330	1.332	1.334	1.318
C2-C9	1.086	1.084	1.526	1.513	1.529	1.516	1.513	1.489
C9-C10			1.194	1.199	1.212	1.216	1.231	1.258
C9-N12(O12)			1.349	1.342	1.362	1.358	1.327	1.325
C1-C2	1.395	1.396	1.402	1.405	1.404	1.408	1.386	1.390
C4-C5	1.394	1.390	1.394	1.392	1.392	1.391	1.384	1.385
RMSD[b]	**0.620**	**0.620**	**0.020**	**0.016**	**0.019**	**0.016**		
RMSD[c]	**0.624**	**0.624**	**0.029**	**0.025**	**0.027**	**0.023**		
			Bond angles (°)					
C2-N3-C4	116.0	117.0	118.6	118.9	118.7	118.8	116.3	116.3
C1-N6-C5	116.0	115.6	116.1	117.0	116.3	117.0	115.9	116.7
C1-C2-N3	121.9	119.9	117.7	118.9	117.7	118.6	121.5	116.3
C5-C4-N3	121.9	121.6	121.5	120.5	121.5	120.8	121.9	123.6
C2-C1-N6	122.0	124.1	125.0	123.0	124.8	123.2	122.3	122.9
C4-C5-N6	121.9	121.5	120.8	121.5	120.7	121.3	122.0	120.3
N6-C1-F11	117.1	117.0	115.1	116.1	114.8	115.6	115.7	125.3
C2-C1-F11	120.8	118.7	119.8	120.8	120.2	121.0	122.0	111.8
N3-C2-C9	117.1	118.7	115.5	116.2	115.2	117.6	118.6	118.3
C1-C2-C9	120.9	121.2	126.6	124.8	127.0	123.6	119.8	121.6
C2-C9-O10			121.5	123.9	120.3	122.5	119.2	119.2
C2-C9-N12(O12)			117.3	113.0	116.7	113.2	116.1	117.2
O10-C9-N12(O12)			121.1	123.0	122.9	124.2	124.7	123.6
RMSD[b]	**0.7**	**1.3**	**2.9**	**2.5**	**0.7**	**1.3**		
RMSD[c]	**4.3**	**3.7**	**4.8**	**5.0**	**4.3**	**3.7**		
			Dihedral angles (°)					
C1-C2-N3-C4	0.0	0.0	-0.0	-0.0	-0.0	-0.0	-0.1	
C2-N3-C4-C5	0.0	0.0	0.0	-0.0	0.3	-0.0	0.0	
N3-C4-C5-N6	0.0	0.0	0.0	0.0	-0.3	0.0	0.0	
C4-C5-N6-C1	0.0	0.0	-0.0	-0.0	-0.0	-0.0	-0.0	
C5-N6-C1-C2	0.0	0.0	0.0	-0.0	0.3	-0.0	-0.0	
N6-C1-C2-N3	0.0	0.0	-0.0	0.0	-0.3	0.0	0.1	
N3-C2-C1-F11	180.0	180.0	-179.9	-179.9	179.7	-179.9	-179.	
N6-C1-C2-C9	180.0	180.0	179.9	-179.9	178.8	-179.9	-179.7	
N3-C2-C9-O10			0.1	-179.9	9.1	-179.9	-178.0	
N3-C2-C9-N12(O12)			-179.8	0.0	-169.8	0.0	2.1	
C1-C2-C9-O10			-179.8	0.0	-170.0	0.0	1.8	
RMSD[b]	**162.4**	**162.4**	**143.7**	**1.1**	**178.7**	**1.1**		

[a]This work, [b]Ref [10] for β form of pyrazincarboxamide ; [c]Ref [11] for δ form of pyrazincarboxamide

STRUCTURAL STUDY IN GAS PHASE

Calculated geometrical parameters for P, FP, FPCOOH and $FPCONH_2$ species by using the B3LYP/6-311++G** level of theory in gas phase can be seen in Table 2 compared with the corresponding experimental ones reported for two and forms of pyrazincarboxamide [10,11] by using the root-mean-square deviation (RMSD) values. In general, the rmsd values corresponding to the bond lengths for P and FP (0.624-0.620 Ĺ) are higher than those observed for FPCOOH and $FPCONH_2$ (0.029-0.016 Ĺ) while for both C2 conformations of these two species there are very good correlations with the experimental ones of the β form. Thus, analyzing the bond lengths of both C2 conformers we observed rmsd values of 0.016 Ĺ while when these parameters are compared with the corresponding to the form the values increase from 0.025 to 0.023 Ĺ. On the other hand, when the calculated and experimental bond lengths values only for FPCOOH and $FPCONH_2$ are compared by a graphic, as that represented in **Figure 4**, it is possible to observe that the C2-C9 and C9-C10 bonds present the higher variations. For the bond angles, the better correlations are obtained when the theoretical values are compared with the experimental ones corresponding to the form (2.9-0.7 ş) but, when the values are compared with the corresponding for the form δ the rmsd values increase significantly from 5.0 to 3.7 ş. These variations only for FPCOOH and $FPCONH_2$ can be clearly seeing when the values are represented in **Figure 5**. Thus, comparing the bond angles of both species we observed that the N3-C2-C9, C1-C2-C9 and C2-C9-O10 angles are slightly different, as expected because the involved distances are different. But the higher differences are observed when the values are compared with the experimental values corresponding to the form. Hence, the high rmsd values can be evidently justified by the experimental values observed for the N6-C1-F11 and C2-C1-F11 angles of 125.3 and 111.8ş, respectively. In relation to the dihedral angles, the lower values are observed for both C2 conformations of FPCOOH and $FPCONH_2$ when the values are compared with the experimental ones for the β form being in both cases of 1.1ş. Here, the dihedral N3-C2-C9-N12 (O12) C1-C2-C9-O10 angles can clearly explain the differences observed of C2 with the C1 conformations of both species.

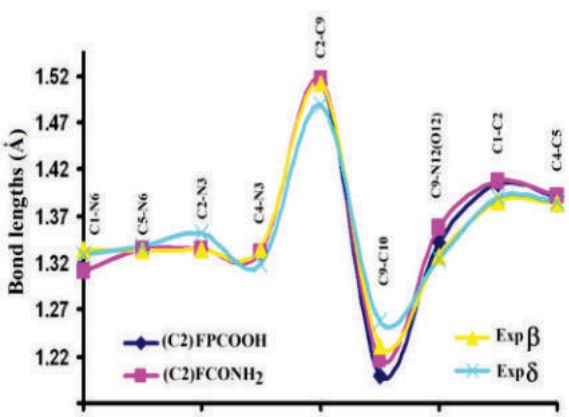

Figure 4. Calculated and experimental bond lengths values for FPCOOH and $FPCONH_2$ species.

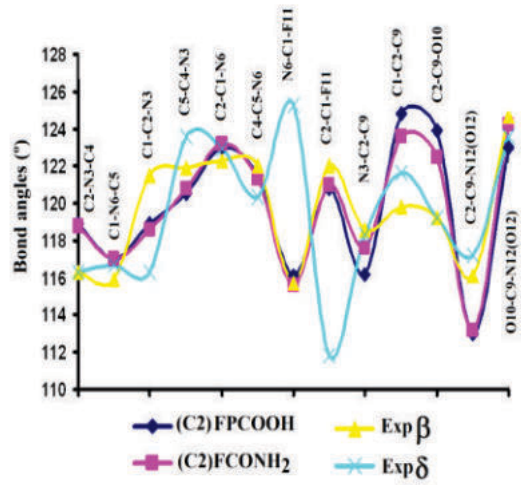

Figure 5. Calculated and experimental bond angles values for FPCOOH and $FPCONH_2$ species.

CHARGES, MOLECULAR ELECTROSTATIC POTENTIALS AND BOND ORDERS STUDIES

The studies related to the charges, molecular electrostatic potentials and bond orders are of great interest in these fluoropyrazine species because they have in their structures F atoms of high electronegativity and different electron's donor and acceptor groups, such as C=O, OH and NH_2. For these reasons, for the four species considered two charge's types were studied in this work, including the two C1 and C2 conformations of FPCOOH and $FPCONH_2$. Hence, MK and NPA charges [19,22], the molecular electrostatic potentials and bond orders calculated for P, FP, FPCOOH and $FPCONH_2$ in gas phase by using the hybrid B3LYP/6-311++G** level of theory are summarized in **Table 3**. First, comparing the MK charges for P and FP, it is observed that the positive charge on the C1 atom belong to the C1-F9 bond increase from 0.191 a.u in P to 0.613 a.u. in FP while the charge on the C2 atom decrease from 0.140 a.u. in P to 0.046 a.u. in FP. In addition, the charges on the N3 and N6 atoms and, on the C4 and C5 atoms also decrease their values due to the effect of replace an H atom by F atom. Now, the effect of change an H atom of FP by a COOH group is the increase in the charge on the C1, C5, N6 and H7 atoms while the MK charges on the C2, N3, C4, H8 and F atoms decrease. On the other side, when on FP an H atom is replaced by the $CONH_2$ group the MK charges on the C1, C2, C5, N6 and H7 atoms increase their values while the charges on the N3, C4, H8 and F atoms slightly decrease. A very important result is the similar MK charges that present the F atoms of both C2 conformers of FPCOOH and $FPCONH_2$ while these charges on the N3 and N6 atoms of C2 corresponding to $FPCONH_2$ present higher values than C2 of the other species. Other important result is that in $FPCONH_2$ the MK charges on the two N atoms have higher values than the F atom while in the carboxylic species the N6 atom present higher charge than the F atom. In relation to the NPA charges, their values are lower than the MK charges but, in particular, the NPA charges on the F atoms corresponding to FP, FPCOOH and $FPCONH_2$ are higher than the corresponding MK

charges. Note that both C1 and C2 conformers of the two species show different MK charges on all atoms while the NPA charges present very similar values, as observed in Table 3. On the other hand, the two N atoms of the three fluorinated species have higher NPA charges than the F atoms, a similar result observed for the MK charges of FP and $FPCONH_2$. This way, the negative MK charges observed on the C2 conformer corresponding to the amide species follow the trend: N12 > N6 > O10 > N3 > F11> C4 while on the C2 conformer of the acid species the trend change at: N6 > O12 > O10 > F11> N3> C4> C2. However, the NPA charges observed on all atoms of both C2 conformers show different tendency, thus, in C2 of amide species the variation is: N12 > N6 > O10 > N3 > F11 while in the same conformer of the acid species change at: O12> O10 > N6 > N3> F11, where clearly the C4 and C2 atoms have positive NPA charges different from those MK charges.

Regarding the molecular electrostatic potentials (MEP) from Table 3 it is observed that the incorporation of the F atom to pyrazine ring in FP generate the diminishing of MEPs values on all atoms of FP. In the same way, when FP is compared with the C2 conformer of both acid and amide species there are also observed decreasing in the MEPs values on all atoms but in particular, on the F atom of the amide species, the value practically do not change.

Hence, these variations are most evident for the acid species. Now, if the surface mapped are represented for all species in Figure 6 it is observed as the coloration range change significantly in all species.

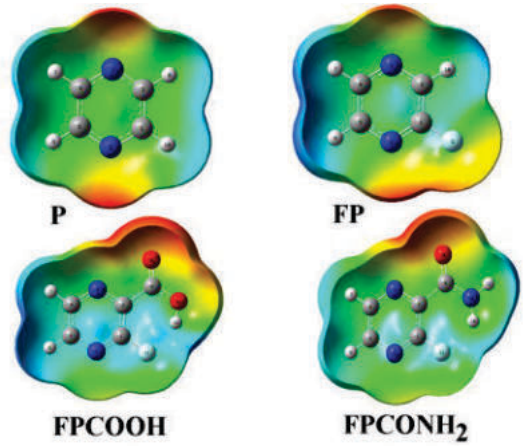

Figure 6. Calculated electrostatic potential surfaces on the molecular surface of P, FP, FPCOOH and $FPCONH_2$ species in gas phase by using the hybrid B3LYP/6-311++G** level of theory. Color ranges, in au: from red -0.062 to blue +0.062. Isodensity value of 0.005.

Thus, when the F atom is incorporated to the pyrazine ring the red colour on the N6 atom is extended in FP and, obviously, the slightly blue colour decrease in that region.

TABLE – 3

Atomic MK and NPA charges, molecular electrostatic potentials and Wiberg indexes for pyrazine (P), F-pyrazine (FP), 3-fluoropyrazine-2-carboxilic acid (FPCOOH) and 3-fluoropyrazine-2-carboxamide ($FPCONH_2$) in gas phase by using the hybrid B3LYP/6-311++G** level of theory.

MK charges									
Atoms	pyrazine	Atoms	F-pyrazine	F-pyrazine-2-carboxil acid			F-pyrazine-2-carboxamide		
				Atoms	C1	C2	Atoms	C1	C2
1 C	0.191	1 C	0.613	1 C	0.511	0.689	1 C	0.593	0.670
2 C	0.140	2 C	0.046	2 C	0.128	-0.007	2 C	0.095	0.088
3 N	-0.443	3 N	-0.423	3 N	-0.390	-0.214	3 N	-0.381	-0.262
4 C	0.142	4 C	0.128	4 C	0.133	-0.120	4 C	0.107	-0.094
5 C	0.187	5 C	0.078	5 C	0.161	0.301	5 C	0.152	0.274
6 N	-0.471	6 N	-0.459	6 N	-0.426	-0.536	6 N	-0.459	-0.544
7 H	0.067	7 H	0.085	7 H	0.075	0.128	7 H	0.077	0.116
8 H	0.061	8 H	0.107	8 H	0.079	0.066	8 H	0.080	0.065
9 H	0.068	9 F	-0.281	9 C	0.591	0.562	9 C	0.741	0.486
10 H	0.059	10 H	0.107	10 O	-0.449	-0.452	10 O	-0.554	-0.501
				11 F	-0.269	-0.256	11 F	-0.304	-0.255
				12 O	-0.549	-0.456	12 N	-1.084	-0.725
				13 H	0.405	0.295	13 H	0.476	0.391
							14 H	0.462	0.291
NPA charges									
Atoms	pyrazine	Atoms	F-pyrazine	Atoms	C1	C2	Atoms	C1	C2
1 C	0.013	1 C	0.576	1 C	0.588	0.624	1 C	0.589	0.619
2 C	0.013	2 C	-0.030	2 C	0.008	0.020	2 C	0.040	0.049
3 N	-0.414	3 N	-0.397	3 N	-0.346	-0.439	3 N	-0.352	-0.424
4 C	0.013	4 C	-0.006	4 C	0.012	0.011	4 C	0.008	0.004
5 C	0.013	5 C	0.026	5 C	0.048	0.049	5 C	0.040	0.041
6 N	-0.414	6 N	-0.441	6 N	-0.429	-0.430	6 N	-0.436	-0.437
7 H	0.194	7 H	0.200	7 H	0.207	0.207	7 H	0.203	0.202
8 H	0.194	8 H	0.199	8 H	0.205	0.205	8 H	0.201	0.201
9 H	0.194	9 F	-0.336	9 C	0.761	0.760	9 C	0.631	0.627
10 H	0.194	10 H	0.208	10 O	-0.520	-0.535	10 O	-0.580	-0.591

				11 F	-0.350	-0.301	11 F	-0.351	-0.305
				12 O	-0.670	-0.666	12 N	-0.798	-0.796
				13 H	0.486	0.496	13 H	0.400	0.400
							14 H	0.404	0.411
MEP									
Atoms	pyrazine	Atoms	F-pyrazine	Atoms	C1	C2	Atoms	C1	C2
1 C	-14.723	1 C	-14.631	1 C	-14.600	-14.603	1 C	-14.616	-14.619
2 C	-14.723	2 C	-14.707	2 C	-14.671	-14.673	2 C	-14.687	-14.689
3 N	-18.381	3 N	-18.367	3 N	-18.347	-18.333	3 N	-18.362	-18.352
4 C	-14.723	4 C	-14.715	4 C	-14.693	-14.688	4 C	-14.707	-14.703
5 C	-14.723	5 C	-14.706	5 C	-14.682	-14.681	5 C	-14.696	-14.696
6 N	-18.381	6 N	-18.365	6 N	-18.340	-18.345	6 N	-18.354	-18.359
7 H	-1.086	7 H	-1.077	7 H	-1.058	-1.050	7 H	-1.071	-1.065
8 H	-1.086	8 H	-1.073	8 H	-1.051	-1.051	8 H	-1.063	-1.064
9 H	-1.086	9 F	-26.569	9 C	-14.617	-14.620	9 C	-14.650	-14.652
10 H	-1.087	10 H	-1.069	10 O	-22.371	-22.370	10 O	-22.395	-22.394
				11 F	-26.532	-26.554	11 F	-26.550	-26.570
				12 O	-22.309	-22.314	12 N	-18.358	-18.362
				13 H	-0.942	-0.951	13 H	-1.002	-1.004
							14 H	-0.997	-1.004
Bond order									
Atoms	pyrazine	Atoms	F-pyrazine	Atoms	C1	C2	Atoms	C1	C2
1 C	3.948	1 C	3.856	1 C	3.852	3.859	1 C	3.852	3.858
2 C	3.948	2 C	3.947	2 C	3.991	3.985	2 C	3.993	3.991
3 N	3.089	3 N	3.098	3 N	3.129	3.103	3 N	3.126	3.097
4 C	3.948	4 C	3.947	4 C	3.939	3.935	4 C	3.941	3.940
5 C	3.948	5 C	3.940	5 C	3.931	3.933	5 C	3.935	3.936
6 N	3.089	6 N	3.119	6 N	3.134	3.124	6 N	3.129	3.122
7 H	0.965	7 H	0.963	7 H	0.960	0.960	7 H	0.962	0.962
8 H	0.965	8 H	0.964	8 H	0.961	0.961	8 H	0.962	0.963
9 H	0.965	9 F	1.046	9 C	3.871	3.875	9 C	3.922	3.923
10 H	0.965	10 H	0.960	10 O	2.106	2.081	10 O	2.034	2.012
				11 F	1.039	1.098	11 F	1.033	1.093
				12 O	2.004	2.013	12 N	3.078	3.083
				13 H	0.768	0.759	13 H	0.843	0.843
							14 H	0.840	0.834

TABLE – 4

Main donor-acceptor energy interactions (in kJ/mol) for pyrazine (P), F-pyrazine (FP), 3-fluoropyrazine-2-carboxilic acid (FPCOOH) and 3-fluoropyrazine-2-carboxamide ($FPCONH_2$) in gas phase by using the hybrid B3LYP/6-311++G** level of theory.

Delocalization	P	FP	FPCOOH		$FPCONH_2$	
			C1	C2	C1	C2
$\sigma C9\text{-}O12 \rightarrow$ LP*(1)H13				44.85		
$\Delta ET_{\sigma \rightarrow LP^*}$				**44.85**		
π (2)C1-C2$\rightarrow\pi^*$N3-C4	23.94					
π (2)C1-C2$\rightarrow\pi^*$C5-N6	23.94					
π (2)N3-C4$\rightarrow\pi^*$C1-C2	28.00					
π (2)N3-C4$\rightarrow\pi^*$ C5-N6	22.59					
π (2) C5-N6 $\rightarrow\pi^*$C1-C2	28					
π (2) C5-N6 $\rightarrow\pi^*$ N3-C4	22.59					
π (2) C1-N6 $\rightarrow\pi^*$C2-N3		65.25	62.83	66.67	62.70	65.20
π (2)C1-N6 $\rightarrow\pi^*$C4-C5		95.47	94.68	101.45	95.10	101.49
π (2) C2-N3 $\rightarrow\pi^*$C1-N6		81.22	89.49	74.82	87.95	76.37
π (2) C2-N3$\rightarrow\pi^*$C4-C5		90.54	89.24	85.60	91.21	88.49
π (2) C2-N3$\rightarrow\pi^*$C9-O10			46.11	49.49	47.28	49.82
π (2)C4-C5$\rightarrow\pi^*$C1-N6		77.04	79.96	74.69	79.88	75.15
π (2)C4-C5$\rightarrow\pi^*$C2-N3		88.57	99.90	98.69	95.81	95.47
$\Delta ET_{\pi \rightarrow \pi^*}$	**149.06**	**498.09**	**562.21**	**551.41**	**559.911**	**551.99**
LP (3) F9$\rightarrow\pi^*$C1-N6		93.72	82.93	107.80	85.40	106.17
LP (2)O10$\rightarrow\pi^*$C2-C9			95.01	89.58	97.23	91.37
LP (2)O10$\rightarrow\pi^*$C9-O12			134.93	132.42		
LP (2)O10$\rightarrow\pi^*$C9-N12					102.12	103.12
LP (2)O12$\rightarrow\pi^*$C9-O10			183.96	194.83		
LP (2)N12$\rightarrow\pi^*$C9-O10					249.92	260.87

$\Delta ET_{LP\rightarrow\pi^*}$		**22.42**	**496.83**	**524.63**	**534.66**	**561.53**
*LP(2)O12→LP(1)*H13*				79.46		
*LP(3)O12→LP(1)*H13*				2199.76		
$\Delta ET_{LP\rightarrow LP^*}$				**2279.22**		
π N3-C4 →π* C1-C2*	158.78					
π C5-N6→π* C1-C2*	158.78					
π C1-N6→π* C2-N3*					1582.26	
π C1-N6→π* C4-C5*		461.39	402.16	517.86	413.03	528.22
π C2-N3→π* C4-C5*		519.20	616.09	450.02	734.64	557.23
π C2-N3→π* C9-O10*			183.04	166.03	216.23	210.17
$\Delta ET_{\pi^*\rightarrow\pi^*}$	**317.56**	**980.59**	**1201.29**	**1133.91**	**2946.15**	**1295.62**
ΔE_{Total}	**466.62**	**1501.10**	**2260.34**	**4534.02**	**4040.72**	**2409.14**

Note that the C9 atom corresponding to the amide species present the higher MEP value than the acid species. Comparing the surface mapped of C2 of FPCOOH and $FPCONH_2$ with the corresponding to FP, it is observed that the red colours on the N6 atoms disappear in both cases increasing the red colours in the superior region, those are, the regions between the N3 atoms and the C=O groups. Hence, these different colours show different reaction sites for the four species where clearly the red and blue colours represent nucleophilic and electrophilic sites while the green colour are clear inactive sites.

When the bond orders (BO), expressed as Wiberg indexes are analyzed for all species from Table 3, it is observed that the BO values for the N3, N6 and F atoms increase in FP, FPCOOH and $FPCONH_2$ having where the higher value is observed for C2 of the acid species. On the other hand, the higher BO corresponding to the C9 atom is observed for the $FPCONH_2$ species than the acid species.

AIM AND NBO STUDIES

The charges, MEP and bond orders studies for the fluorinated pyrazine species have evidenced important changes when the F atom or the COOH or $CONH_2$ groups are incorporated to the pyrazine ring. Hence, it is necessary to analyze if these changes generate some modifications in the stability of these species. For these reasons, the donor-acceptor energy interactions and the topological properties were studied for these species by using the NBO and AIM calculations [19-21]. These properties for all species in gas phase by using the hybrid B3LYP/6-311++G** level of theory can be seen in **Table 4**. Therefore, the NBO and the AIM2000 programs were employed together with the Bader's theory to compute those properties [19-21]. The analysis of the donor-acceptor energy interactions calculated with the NBO program [19] show that in P and FP there are two common $\Delta ET_{\pi\rightarrow\pi^*}$ and $\Delta ET_{\pi^*\rightarrow\pi^*}$ interactions but, in particular, when the F atom is incorporated to the pyrazine ring in FP appear a new $\Delta ET_{LP\rightarrow\pi^*}$ interaction which produces a significant increase in the total energy of FP. Then, FP is most stable than P. If now the acid and amide species are compared with FP, it is observed that the acid species is most stable than amide species because the acid species presents two new $\Delta ET_{\sigma\rightarrow LP^*}$ and $\Delta ET_{LP\rightarrow LP^*}$ interactions not observed in the amide species. Thus, the C2 acid species is significantly most stable than the amide species with a total energy value of 4534.02 kJ/mol while the total energy for C2 of the amide species is 2409.14 kJ/mol. These studies support clearly the high stability of the acid species, as compared with the amide species and also, of FP than P.

The topological properties for P, FP, FPCOOH and $FPCONH_2$ were computed in gas phase with the AIM study [20,21] by using the hybrid B3LYP/6-311++G** level of theory. Here, the electron density, $\rho(r)$, the Laplacian values, $\nabla^2\rho(r)$, the eigenvalues $(\lambda1, \lambda2, \lambda3)$ of the Hessian matrix and, the $|\lambda1|/\lambda3$ ratio were computed in the bond critical points (BCPs) and ring critical points (RCPs), in accordance with the Bader's theory [21].

This theory says that if $|\lambda1|/\lambda3 < 1$ and $\nabla^2\rho(r) > 0$ there is H bonds formation [40]. The results for P and FP can be seen in **Table 5**. In both species there is not H bonds formed and, only the properties for the pyrazine rings (RCP1) were considered. Note that a slight higher electron density is observed for FP.

TABLE – 5

Analysis of the topological properties for pyrazine (P) and F-pyrazine (FP) in gas phase by using the hybrid B3LYP/6-311++G** level of theory.

Parameter (a.u.)	Pyrazine RCP1	F-Pyrazine RCP1
$\rho(r_c)$	0.0261	0.0265
$\nabla^2\rho(r_c)$	0.1912	0.1920
λ_1	-0.0237	-0.0241
λ_2	0.0962	0.1006
λ_3	0.1187	0.1156
$\lvert\lambda_1\rvert/\lambda_3$	0.1997	0.2085

This theory says that if $|\lambda1|/\lambda3 < 1$ and $\nabla^2\rho(r) > 0$ there is H bonds formation [40]. The results for P and FP can be seen in **Table 5**. In both species there is not H bonds formed and, only the properties for the pyrazine rings (RCP1) were considered.

Note that a slight higher electron density is observed for FP.

TABLE – 5

Analysis of the topological properties for pyrazine (P) and F-pyrazine (FP) in gas phase by using the hybrid B3LYP/6-311++G** level of theory.

Parameter (a.u.)	Pyrazine RCP1	F-Pyrazine RCP1
$\rho(r_c)$	0.0261	0.0265
$\nabla^2\rho(r_c)$	0.1912	0.1920
λ_1	-0.0237	-0.0241

λ_2	0.0962	0.1006
λ_3	0.1187	0.1156
$\lvert\lambda_1\rvert/\lambda_3$	0.1997	0.2085

However, when the values are analyzed, for C1 of both species from **Table 6**, it is observed halogen bonds formations en FPCOOH and $FPCONH_2$ and, for these reasons, the new RCPs formed are named RCPN.

TABLE – 6

Analysis of the topological properties for the C1 conformers of 3-fluoropyrazine-2-carboxilic acid (FPCOOH) and 3-fluoropyrazine-2-carboxamide ($FPCONH_2$) in gas phase by using the hybrid B3LYP/6-311++G** level of theory.

	3-fluoropyrazine-2-carboxilic acid		
	F11---H13	RCPN	RCP1
$\rho(r_c)$	0.0273	0.0141	0.0269
$\nabla^2\rho(r_c)$	0.1080	0.0800	0.1924
λ_1	-0.0390	-0.0127	-0.0247
λ_2	-0.0383	0.0369	0.1035
λ_3	0.1853	0.0556	0.1136
$\lvert\lambda_1\rvert/\lambda_3$	0.2105	0.2284	0.2174
Distance	1.864		
Parameter (a.u.)	3-fluoropyrazine-2-carboxamide		
	F11---H14	RCPN	RCP1
$\rho(r_c)$	0.0207	0.0114	0.0268
$\nabla^2\rho(r_c)$	0.0875	0.0694	0.1920
λ_1	-0.0259	-0.0086	-0.0246
λ_2	-0.0248	0.0286	0.1036
λ_3	0.1382	0.0492	0.1131
$\lvert\lambda_1\rvert/\lambda_3$	0.1874	0.1748	0.2175
Distance	2.010		

Here, the properties for the acid species are higher than for the amide species. If later, it is analyzed the properties for both C2 conformers of FPCOOH and $FPCONH_2$ from **Table 7**, two new N---H and F---O interactions are observed, hence, two new rings are observed RCPN1 and RCPN2. The properties of N---H for the acid species are higher than the observed in the amide species but, on the contrary, the properties of the F---O interaction is higher for the amide species. Thus, the existence of this interaction in C2 could justify the low stability that presents the amide species because the electronegativities of both atoms produce a higher repulsion in the amide species due to their lower F-O distance (2.741 Ĺ), as compared with the acid species (2.796 Ĺ).

This AIM study evidence clearly the high stabilities of both C2 conformers of the acid and amide species due to the formation of H and halogen bonds where the high density observed for the H bonds of the acid species suggest a high stability of this species than the amide ones while the halogen bond is stronger for the amide species than the acid ones due to their lower distance.

FRONTIER ORBITALS AND DESCRIPTORS STUDIES

According to Parr and Pearson [23], the highest occupied molecular orbital (HOMO) and the lowest unoccupied molecular orbital (LUMO) are parameters useful to predict the reactivities and behaviours of diverse species in different media.

Thus, the evaluations of these orbitals for the fluorinated species are of great interest knowing that it is indispensable the design of new and better drugs for the treatment of tuberculosis. The gap values can be easily calculated from the differences between those two orbitals. Thus, in Table 8 it is presented the frontier orbitals together with the gap values for all studied species in gas phase by using the hybrid B3LYP/6-311++G** level of theory.

TABLE – 7

Analysis of the topological properties for the C2 conformers of 3-fluoropyrazine-2-carboxilic acid (FPCOOH) and 3-fluoropyrazine-2-carboxamide ($FPCONH_2$) in gas phase by using the hybrid B3LYP/6-311++G** level of theory.

3-fluoropyrazine-2-carboxilic acid					
Parameter (a.u.)	N3---H13	RCPN1	F11---O10	RCPN2	RCP1
$\rho(r_c)$	0.0279	0.0246	0.0109	0.0107	0.0263
$\nabla^2\rho(r_c)$	0.0995	0.1456	0.0444	0.0527	0.1900
λ_1	-0.0348	-0.0253	-0.0097	-0.0089	-0.0241
λ_2	-0.0284	0.0396	-0.0058	0.0079	0.1057
λ_3	0.1628	0.1313	0.0599	0.0537	0.1084
$\lvert\lambda_1\rvert/\lambda_3$	0.2138	0.1927	0.1619	0.1657	0.2223
Distance (Ĺ)	2.009		2.796		
3-fluoropyrazine-2-carboxamide					
Parameter (a.u.)	N3---H14	RCPN1	F11---O10	RCPN2	RCP1
$\rho(r_c)$	0.0182	0.0179	0.0123	0.0116	0.0263
$\nabla^2\rho(r_c)$	0.0814	0.1023	0.0490	0.0600	0.1899
λ_1	-0.0174	-0.0153	-0.0110	-0.0096	-0.0240
λ_2	-0.0088	0.0114	-0.0086	0.0128	0.1052
λ_3	0.1077	0.1062	0.0687	0.0568	0.1086
$\lvert\lambda_1\rvert/\lambda_3$	0.1616	0.1441	0.1601	0.1690	0.2210
Distance (Ĺ)	2.254		2.741		

TABLE – 8

Calculated HOMO and LUMO orbitals and energy band gap (eV) for pyrazine, F-pyrazine, 3-fluoropyrazine-2-carboxilic acid and 3-fluoropyrazine-2-carboxamide in gas phase by using the hybrid B3LYP/6-311++G** level of theory.

Species	HOMO	LUMO	GAP
P	-7,1729	-1,8885	-5,2844
FP	-7,7770	-2,1851	-5,5919
Acid C1	-8,1444	-3,0885	-5,0559
Acid C2	-8,0665	-3,1501	-4,9164
Amide C1	-7,5566	-2,6368	-4,9198
Amide C2	-7,4317	-2,6958	-4,7359

First, comparing the gap values of P and FP it is observed that the presence of the F atom in FP increases the gap value from -5.2844 eV in P to -5.5919 eV in FP and, as a consequence, decrease the reactivity of FP while the carboxyl and carboxamide groups increase the reactivity of FP because in both cases the gap values decrease, being most reactive the amide species due to their lower gap value. On the other hand, the two C2 species of FPCOOH and FPCONH$_2$ are most reactive than the corresponding C1 ones, as observed in Table 8. When the descriptors for pyrazine are compared with those calculated for F-pyrazine it is observed a clear increase in the electrophilicity and nucleophilicity indexes, as indicated in Table 9. Obviously, the global hardness in FP increases according to the decreasing of their reactivity, as compared with P.

TABLE – 9

Calculated chemical potential (μ). electronegativity (χ). global hardness (η). global softness (S). global electrophilicity index (ω) and global nucleophilicity index (E) (eV) for pyrazine and F-pyrazine.

Descriptors (eV)	Pyrazine	F-Pyrazine
χ	-2.6422	-2.7960
μ	-4.5307	-4.9810
η	2.6422	2.7960
S	0.1892	0.1788
ω	3.8845	4.4369
E	-11.9710	-13.9269

$\chi = -[E(LUMO) - E(HOMO)]/2$; $\mu = [E(LUMO) + E(HOMO)]/2$;

$\eta = [E(LUMO) - E(HOMO)]/2$; $S = \frac{1}{2}\eta$; $\omega = \mu^2/2\eta$; $E = \mu * \eta$

Table 10 shows the descriptors calculated for the acid and carboxamide species in gas phase by using the hybrid B3LYP/6-311++G** level of theory.

TABLE – 10

Calculated chemical potential (μ). electronegativity (χ). global hardness (η). global softness (S). global electrophilicity index (ω) and global nucleophilicity index (E) (eV) for 3-fluoropyrazine-2-carboxilic acid and 3-fluoropyrazine-2-carboxamide.

Descriptors (eV)	F-pyrazine-2-carboxil acid		F-pyrazine-2-carboxamide	
	C1	C2	C1	C2
χ	-2.5279	-2.4582	-2.4599	-2.3680
μ	-5.6164	-5.6083	-5.0967	-5.0638
η	2.5279	2.4582	2.4599	2.3680
S	0.1978	0.2034	0.2033	0.2112
ω	6.2391	6.3976	5.2799	5.4143
E	-14.1980	-13.7863	-12.5374	-11.9907

The results of Table 10 shows clearly the increase in the global softness values of both C2 acid and amide species while their global hardness values decrease conform their reactivities increase. Note that the electrophilicity indexes of both C1 and C2 acid species are higher than the corresponding to the amide ones. These results are in agreement with the molecular electrostatic potential values of the COOH and CONH$_2$ groups observed from Table 3 because in the acid species there are two O atoms with higher MEP values than the amide species (O and N atoms).

VIBRATIONAL ANALYSIS

The assignments of the vibrational spectra for pyrazine were already reported by Breda et al. [15] and by Schmitt et al. [16] and, for these reasons, in this work the bands observed in the infrared spectra of P were taken of those two publications. Here, the tentative assignments for FP, FP-COOH and FP-CONH$_2$ were presented considering their optimized C_s structures and the corresponding force fields computed with the SQMFF methodology [28] and the Molvib program [29]. The internal coordinates for those species were similar to those reported in the literature for species with related groups [33-36]. Only, the theoretical assignments for the C2 conformers of both acid and amide species were presented in Table 11 together with the assignments for the other species. The scaled force fields were calculated by using the hybrid B3LYP/6-311++G** level of theory and taking into account the scale factors reported by Rauhut and Pulay [28]. The complete assignments for all species were performed using the potential energy distribution (PED) contributions 10 %. The predicted infrared spectra for P, FP, FP-COOH and FP-CONH$_2$ species in gas phase by using B3LYP/6-311++G** level of theory are presented in Figure 7 compared with the experimental available for P taken from Ref [16] while the predicted Raman spectra of all species are presented in Figure 8. The theoretical activities of all Raman spectra were transformed to intensities by using recognized equations [40,41]. At this point, brief discussions on the assignments performed for each species are presented at continuation.

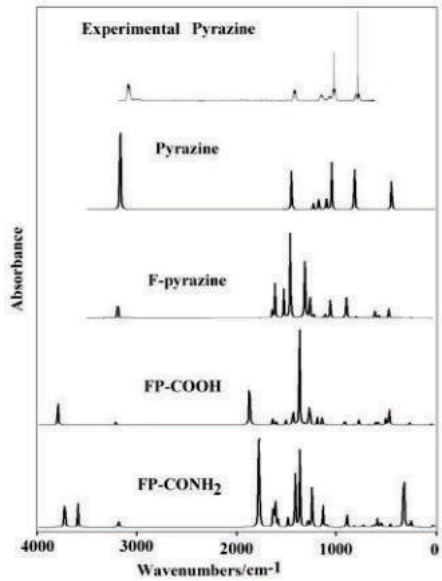

Figure 7. Experimental available infrared spectrum of pyrazine (from Ref [16]) compared with the corresponding predicted for pyrazine, fluoro-pyrazine, 3-fluoropyrazine-2-carboxilic acid and 3-fluoropyrazine-2-carboxamide in gas phase by using the hybrid B3LYP/6-311++G** level of theory.

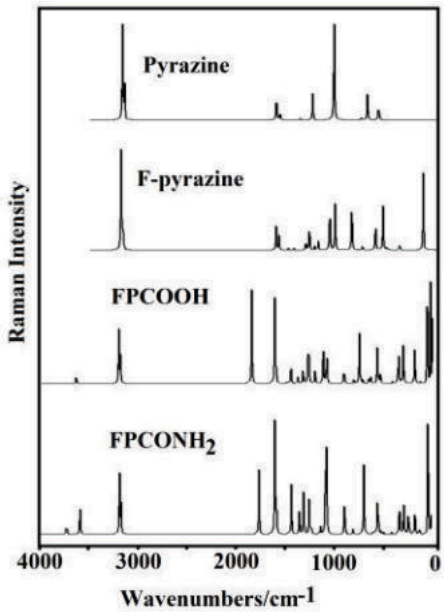

Figure 8. Predicted Raman spectra for pyrazine, fluoro-pyrazine, 3-fluoropyrazine-2-carboxilic acid and 3-fluoropyrazine-2-carboxamide in gas phase by using the hybrid B3LYP/6-311++G** level of theory.

ASSIGNMENTS

Pyrazine. The SQM/B3LYP/6-311++G** calculations predicted all vibration modes as was previously reported [15,16]. In this work, the vibration modes were clearly specified in accordance to the higher PED contributions observed for each mode. Thus, the CH stretching modes were predicted between 3041 and 3020 cm^{-1} while the corresponding deformation in-plane and out-of-plane were predicted between 1467/1215 and 978/792 cm^{-1}, as indicated in Table 11. In the higher wavenumbers region it is predicted a strong IR band assigned to the CH stretching modes.

Skeletal vibrations, such as the C1=C2 and C4=C5 stretching modes are assigned to the IR band observed at 1579 cm^{-1} while the C2=N3 and C5=N6 are associated to the IR band located at 1522 cm^{-1}.

TABLE – 11

Observed and calculated wavenumbers (cm^{-1}) and assignments for for pyrazine, F-pyrazine, 3-fluoropyrazine-2-carboxilic acid and 3-fluoropyrazine-2-carboxamide in gas phase.

Experimental		B3LYP/6-311++G** method[a]							
		Pyrazine		F-pyrazine		F-pyrazine-2-carboxil		F-pyrazine-2-	
IR[c]	IR[d]	SQM[b]	Assignments	SQM[b]	Assignments	SQM[b]	Assignments	SQM[b]	Assignments
						3479	νO12-H13	3570	$\nu_a NH_2$
3069	3069	3041	νC2-H9	3054	νC4-H7	3062	νC4-H7	3438	$\nu_s NH_2$
3062	3055	3035	νC5-H8	3049	νC2-H10	3044	νC5-H8	3055	νC4-H7
3053	3040	3022	νC1-H10	3036	νC5-H8			3038	νC5-H8
	3018	3020	νC4-H7						
						1772	νC9-O10	1702	νC9-O10
1579	1580	1560	νC1-C2	1563	νC1-C2	1554	νC1-C2,	1552	νC1-N6
1522	1525	1523	νC2-N3	1533	νC2-N3	1534	νC5-N6	1531	νC5-N6
								1520	δNH_2
1484	1483	1467	βC2-H9	1454	βC5-H8	1437	βC4-H7	1435	βC4-H7
1413	1413	1397	βC4-H7	1390	βC4-H7	1396	νC1-C2	1390	νC1-C2
1353	1346	1337	βC4-H7			1338	δC9O12H13		
								1314	νC9-N12
				1282	βC5-H8	1279	νC1-F11	1271	νC1-F11
				1245	νC1-F9	1226	νN3-C4		
1235	1233	1215	βC4-H7			1215	νC2-N3	1214	νC2-N3
1174		1170	νN3-C4	1188	νC5-N6			1190	νN3-C4
1135	1135	1134	βR_1	1156	νN3-C4	1161	νC1-N6	1115	βR_1, νC1-N6
						1078	νC9-O12		
1063	1063	1051	νC1-C2	1042	νC4-C5	1048	νC4-C5	1054	νC4-C5
1020	1020	1023	βR_1	1010	βR_1			1041	ρNH_2
1015	1016	998	νC4-C5						
982	971	978	γC1-H10						
976	960	971	γC2-H9	967	γC5-H8	971	γC5-H8	968	γC5-H8
925	927	929	γC4-H7	926	γC2-H10	894	βR_1	891	βR_1
				853	γC4-H7	870	γC4-H7	869	γC4-H7
				844	νC1-F9, βR_2				
785	785	792	γC5-H8			798	τR_1	807	τR_1, γC2-C9
755	756	747	τR_1	740	τR_1	742	δCOO,		
698	704	715	βR_2			709	τR_1, γCOO	713	τR_1,γC9=O10

				634	βR_2	649	βR_2	698	βR_2
								625	δO10C9N12
596	602	609	βR_3			604	τOH		
				567	βR_3	586	βR_3	583	βR_3
						559	βC1-F11	557	τwNH_2
				526	γC1-F9	549	γC1-F11	542	τR_2, γC1-F11
								530	βC1-F11
				423	τR_2	445	τR_2	449	τR_2, γC2-C9
417	418	419	τR_2	422	βC1-F9				
						397	ρCOO	390	ρO10C9N12
						353	βC1-F11	350	βC1-F11,
338	336	336	τR_3					307	γNH_2
						249	γC2-C9	248	γC2-C9
				204	τR_3	198	βC2-C9	205	βC2-C9
						112	τR_3	106	τR_3
						57	τwCOO	27	τwCON

Abbreviations: ν, stretching; β, deformation in the plane; γ, deformation out of plane; wag, wagging; τ, torsion; β_R, deformation ring; τ_R, torsion ring; ρ, rocking; τw, twisting; δ, deformation; a, antisymmetric; s, symmetric; [a]This work, [b]From scaled quantum mechanics force field; [c]From Ref [15]; [d]From Ref [16].

The remaining C-C and C-N stretching modes can be clearly associated to the IR bands observed between 1170 and 998 cm^{-1}. The three deformations and torsion rings can easily be assigned as predicted by the SQM calculations. Thus, the deformations ring are predicted coupled with some stretching modes while the torsion rings are predicted in the those regions expected for six members rings [33,34,36,37].

F-Pyrazine. The only difference observed in the vibrational spectra of FP, in relation to pyrazine, is the presence of the C-F bond, hence, it is expected the stretching, in-plane and out-of-plane deformation modes related to that bond. Here, the stretching mode is predicted at 1245 cm^{-1} and, also appear coupled with one deformation ring mode at lower wavenumbers (844 cm^{-1}). Then, the in-plane and out-of-plane deformation modes can be assigned as predicted by SQM calculations, that is, at 422 and 526 cm^{-1}, as observed in Table 11.

FP-COOH. The difference of this acid species with FP is the presence of the carboxyl group, hence, the additional vibration modes expected for this species are, the OH, C=O and C-O stretching modes, the OH deformation and torsion modes and, the COO deformation, rocking, out-of-plane and twisting modes. The C=O and C-O modes are predicted respectively at 1772 and 1078 cm^{-1} while the OH deformation mode is predicted at 1338 cm^{-1}.

The COO deformation, rocking, out-of-plane and twisting modes are predicted at 798, 397, 709 and 57 cm^{-1}. The C-F stretching mode for this species is predicted at 1279 cm^{-1} while the in-plane and out-of-plane deformation modes are predicted by SQM calculations at 353 and 549 cm^{-1}, as observed in Table 11.

FP-$CONH_2$. The vibration modes related to the NH_2 groups are expected in this amide species [42]. Hence, two NH_2 stretching, deformation, rocking and twisting modes and, also the vibration mode associated to the O10-C9-N12 angles are expected. Thus, these NH_2 stretching modes are predicted by SQM calculations at 3570 and 3438 cm^{-1} while the deformation, rocking and twisting modes are predicted at 1520, 1041 and 557 cm^{-1}, respectively. In this species, the vibration modes related to the C-F group stretching mode for this species is predicted at 1279 cm^{-1} while the in-plane and out-of-plane deformation are predicted at 1271

FORCE CONSTANTS

The harmonic force constants for P, FP, FPCOOH and FP$CONH_2$ were calculated in gas phase from their corresponding force fields at the B3LYP/6-311++G** level of theory. The internal coordinates, the SQMFF methodology [28] and the Molvib program [29] were used to obtain the harmonic force fields. The scaled internal force constants are summarized in **Table 12**. Here, for the acid and amide species were presented only the force constants for the C2 conformers.

TABLE – 12

Comparison of main scaled internal force constants for pyrazine (P), F-pyrazine (FP), 3-fluoropyrazine-2-carboxilic acid (FPCOOH) and 3-fluoropyrazine-2-carboxamide (FP$CONH_2$) in gas phase by using the hybrid B3LYP/6-311++G** level of theory.

Force constants	B3LYP/6-311++G**[a]			
	P	FP	FP-COOH	FP-$CONH_2$
f(ν O-H)			6.76	
f(ν N-H)				6.82
f(ν C-H)	5.03	5.09	5.11	5.09
f(ν C-N)	7.03	7.21	7.24	7.21
f(ν C-C)	6.17	6.21	6.15	6.14
f(ν C-F)		5.59	6.10	6.03
f(νC-CR)			4.02	3.94
f(ν C=O)			12.52	11.39
f(ν C-O)			5.87	
f(ν C-NH_2)				6.47
f(δ NH_2)				0.41
f(δ COOH)			0.85	

Units are mdyn $Å^{-1}$ for stretching and mdyn Å rad^{-2} for angle deformations. [a]This work

First, when the *f(νC-H), f(νC-N),* and *f(νC-C)* force constants are compared for P and FP it is observed that the values of those three constants increase their values as a

consequence of to change the H atom by F, observing this way a higher variation in the *f(νC-N)* force constant for FP. On the other hand, the higher *f(νC-H)* and *f(νC-N)* values are observed for the acid species while the lower *f(νC-C)* force constant value is observed for the amide species. These observations are in agreement with the calculated parameters, as shown in Table 2. Hence, the lower C-H and C-N bond lengths observed for the acid species and the longer C-C distances observed in the amide species justify such modifications. The *f(ν C-F)* force constant value is higher in the acid species probably because the C-F distance is lower in that species than the other ones. In relation to the *f(ν C=O)* force constant value, it is observed that is higher in the acid species than the amide one because the C=O distance is shorter in this acid species than the amide one.

CONCLUSIONS

In this work, the structures of F-pyrazine, 3-fluoropyrazine-2-carboxilic acid and 3-fluoropyrazine-2-carboxamide were determinate in gas phase by using the hybrid B3LYP/6-311++G** level of theory. Two conformations were found for both acid and amide species being the C2 conformations the most stable than the C1 ones, both with C_S symmetries. Probably, their stabilities are related to their higher dipole moment values, as was reported in the literature for other species. The geometrical parameters show lower RMSD values when they are compared with the experimental values observed for the β form of pyrazincarboxamide than the corresponding to the δ form. In relation to the MK charges, for the amide species are observed higher values on the two N atoms of the pyrazine rings than the acid one. The different colorations observed on the MEP surfaces mapped suggest different nucleophilic and electrophilic sites in the four studied species being higher the region nucleophilic for the acid species, in accordance with the higher nucleophilicity and electrophilicity indexes observed for this species. The NBO study reveals the high stabilities of both acid and amide species especially for the acid species because it presents two new $\Delta ET_{\sigma \rightarrow LP^*}$ and $\Delta ET_{LP \rightarrow LP^*}$ interactions not observed in the amide species. The AIM analysis also supports the high stabilities of both C2 conformers due to the halogen bonds formation observed in both species where the topological properties are higher for the acid species, in very good concordance with the higher total energy observed by NBO calculations. The frontier orbitals predict a low reactivity for FP but higher reactivities for the acid and amide species, being the amide species most reactive than the acid one. The descriptors evidence the higher nucleophilicity and electrophilicity indexes for the acid species than the amide one. The vibrational analyses show that the C=O and C-F stretching modes in the acid species are predicted at higher wavenumbers than the other species. On the other hand, the C2-N3 stretching mode in FP is predicted at higher wavenumbers than pyrazine while in the acid and amide species this stretching mode is predicted with partial double bond at lower wavenumbers (1215-1214 cm^{-1}). The force constants calculated for all species show that their values are strongly related to their geometrical parameters values.

ACKNOWLEDGEMENTS

This work was supported with grants from CIUNT Project Nş 26/D207 (Consejo de Investigaciones, Universidad Nacional de Tucumán). The authors would like to thank Prof. Tom Sundius for his permission to use MOLVIB.

REFERENCES:

[1] Esfahanizadeh, M.; Omidi, K.; Kauffman, J.; Gudarzi, A.; Zahedani, S.S.; Amidi, S.; Kobarfard, F. (2014). Synthesis and Evaluation of New Fluorinated Anti-Tubercular Compounds, Services, Iranian Journal of Pharmaceutical Research 13 (1) ,115-126.
[2] Ugwu, D.I.; Ezema, B.E.; Eze, F.U.; Ugwuja, D.I. (2014). Synthesis and Structural Activity Relationship Study of Antitubercular Carboxamides, International Journal of Medicinal Chemistry, 2014, Article ID 614808, 1-18.
[3] Wade, M.M.; Zhang, Y. (2006). "Effects of weak acids, UV and proton motive force inhibitors on pyrazinamide activity against Mycobacterium tuberculosisin vitro," Journal of Antimicrobial Chemotherapy, 58(5), 936–941.
[4] Dole˘zal, M.; Zitko, J.; Ke˘setovi˘cov´a, D.; Kune˘s, J.; Svobodov´a, M. (2009). "Substituted N-phenylpyrazine-2-carboxamides: synthesis and antimycobacterial evaluation," Molecules, 14(10), 4180–4189.
[5] Martin, D.; Jan, Z.; Carillo C. et al., "Substituted N-benzylpyrazine-2-carboxamides, their synthesis, hydro-lipophilic properties and evaluation of their antimycobacterial and photosynthesis-inhibiting activity," in Proceedings of the 15th International Conference on Synthetic Organic Chemistry, 2011.
[6] Semelkova, L.; Konecna, K.; Paterova, P.; Kubicek, V.; Kunes, J.; Novakova, L.; Marek, J.; Naesens, L.; Pesko, M.; Kralova, K.; Dolezal, M.; Zitk, J. (2015). Synthesis and Biological Evaluation of N-Alkyl-3-(alkylamino)-pyrazine-2-carboxamides, Molecules 20, 8687-8711.
[7] Tůmová, L.; Tůma, J.; Doležal, M.; Jan Kubeš, Z. (2016). New Synthetic Pyrazine Carboxamide Derivatives as Potential Elicitors in Production of Secondary Metabolite in In vitro Cultures, Pharmacogn Mag. 12, S57-62.
[8] Semelková, L.; Jand'ourek, O.; Kone˘cná, K.; Paterová, P.; Navrátilová, L.; Trejtnar, F.; Kubí˘cek, V.; Kuneš, J.; Doležal, M.; Zitko, J. (2017). 3-Substituted N-Benzylpyrazine-2-carboxamide Derivatives: Synthesis, Antimycobacterial and Antibacterial Evaluation, Molecules 22, 495.
[9] Wheatley, P.J. (1957). The Crystal and Molecular Structure of Pyrazine, Acta Cryst. 10, 182-187.
[10] Ro, G.; Sorum, H. (1972). The Crystal and Molecular Structure of -Pyrazincarboxamide, Acta Cryst. B28, 991-998.
[11] Ro, G.; Sorum, H. (1972). The Crystal and Molecular Structure of □-Pyrazincarboxamide, Acta Cryst. B28, 1677-1684.
[12] Leiserowitz, L. (1976). Molecular Packing Modes. Carboxylic Acids, Acta Cryst. B32, 775-802.
[13] Wadt, W.R.; Goddard lll, W.A.; Dunning, Jr., T.H. (1976). The electronic structure of pyrazine. Configuration interaction calculations using an extended basis, The Journal of Chemical Physics, 65(1), 438-445.
[14] Berezin, K.V.; Nechaev, V.V.; El'kin, P.M. (2005). Anharmonic resonances in the vibrational spectra of pyrazine, Journal of Applied Spectroscopy, 72(1) 9-.
[15] Breda, S.; Reva, I.D.; Lapinski, L.; Nowak, M.J.; Fausto, R. (2006). Infrared spectra of pyrazine, pyrimidine and pyridazine in solid argon, Journal of Molecular Structure 786, 193–206.
[16] Schmitt, M.; Biemann, L.; Meerts, W.L.; Kleinermanns, K. (2009). Analysis of the FTIR spectrum of pyrazine using evolutionary algorithms, Journal of Molecular Spectroscopy 257, 74–81.
[17] Prasad, M.V.S.; Sri, N.U.; Veeraiah, A.; Veeraiah, V.; Chaitanya K. (2013) Molecular structure, vibrational spectroscopic (FTIR, FT-Raman),UV-Vis spectra, first order hyperpolarizability, NBO analysis, HOMO and LUMO analysis, thermodynamic properties of 2,6-dichloropyrazine by ab inito HF and density functional method, J. At. Mol. Sci. 4(1), 1-17.
[18] Joseph, T.; Varghese, H.T.; Panicker, C.Y.; Viswanathan, K.; Dolezal, M.; Van Alsenoy, C. (2017). Spectroscopic (FT-IR, FT-Raman), first order hyperpolarizability, NBO analysis, HOMO and LUMO analysis of N-[(4-(trifluoromethyl) phenyl]pyrazine-2-carboxamide by density functional methods, Arabian Journal of Chemistry 10, S2281–S2294.
[19] Glendening, E.D.; Badenhoop, J.K.; Reed, A.D.; Carpenter, J.E.; Weinhold, F. NBO 3.1; Theoretical Chemistry Institute, University of Wisconsin; Madison, WI, 1996.
[20] Biegler-Köning, F.; Schönbohm, J.; Bayles, D. (2001). AIM2000; A Program to Analyze and Visualize Atoms in Molecules, J. Comput. Chem. 22, 545.
[21] Bader, R.F.W. Atoms in Molecules, A Quantum Theory, Oxford University Press, Oxford, 1990, ISBN: 0198558651.
[22] Besler, B.H.; Merz Jr, K.M.; Kollman, P.A. (1990). Atomic charges derived from demiempirical methods, J. Comp. Chem. 11, 431-439.
[23] Parr, R.G.; Pearson, R.G. (1983). Absolute hardness: companion parameter to absolute electronegativity, J. Am. Chem. Soc. 105, 7512-7516.
[24] Brédas, J-L (2014). Mind the gap!, Materials Horizons 1, 17–19.
[25] Romani, D.; Tsuchiya, S.; Yotsu-Yamashita, M.; Brandán, S.A. (2016). Spectroscopic and structural investigation on intermediates species structurally associated to the tricyclic bisguanidine compound and to the toxic agent, saxitoxin, J. Mol. Struct. 1119, 25-38.
[26] Romani, D.; Márquez, M.J.; Márquez, M.B.; Brandán, S.A. (2015). Structural, topological and vibrational properties of an isothiazole derivatives series with antiviral activities, J. Mol. Struct. 1100, 279-289.
[27] Chain, F.; Iramain, M.A.; Grau, A.; Catalán, C.A.N.; Brandán, S.A. (2016). Evaluation of the structural, electronic, topological and vibrational properties of N-(3,4-dimethoxybenzyl)-hexadecanamide isolated from Maca (Lepidium meyenii) using different spectroscopic techniques, J. Mol. Struct. 1119, 25-38.
[28] a) Rauhut, G.; Pulay, P. (1995) J. Phys. Chem. 99 3093-3099. b) Correction: G. Rauhut, P. Pulay, J. Phys. Chem. 99 (1995) 14572.
[29] Sundius, T. (2002). Scaling of ab initio force fields by MOLVIB, Vib. Spectrosc. 29, 89-95.
[30] Nielsen, A.B.; Holder, A.J. Gauss View 3.0, User's Reference, GAUSSIAN Inc., Pittsburgh, PA, 2000–2003.
[31] Frisch, M.J. et al., GAUSSIAN 09, Revision A.02, Gaussian, Inc., Wallingford, CT, 2009.
[32] Ugliengo, P. MOLDRAW Program, University of Torino, Dipartimento Chimica IFM, Torino, Italy, 1998.
[33] Romano, E.; Raschi, A.B.; Benavente, A.M.; Brandán, S.A. (2011). Structural analysis, vibracional spectra and coordinated normal of 2R-(-)-6-hydroxytremetone, Spectrochim. Acta Part A Mol. Biomol. Spectrosc. 84, 111-116.
[34] Romano, E.; Castillo, M.V.; Pergomet, J.; Zinczuk, J.; Brandán, S.A. (2013).

Synthesis, structural study and spectroscopic characterization of a quinolin-8-yloxy derivative with potential biological properties, Open J. Synthesis Theory Appl. 2, 8-22.

[35] Romano, E.; Ladetto, F.; Brandán, S.A. (2013). Structural and vibrational studies of the potential anticancer agent, 5-difluoromethyl-1,3,4-thiadiazole-2-amino by DFT calculations, Comput. Theor. Chem. 1011, 57-64.

[36] Romano, E.; Brandán, S.A. (2016). Vibrational analysis of the tautomers of the adrenergic agonist clonidine agent and their protonated species, ChemXpress 9(2), 192-205.

[37] Romano, E.; Davies, L.; Brandán, S.A. (2017), Structural properties and FTIR-Raman spectra of the anti-hypertensive clonidine hydrochloride agent and their dimeric species, Journal of Molecular Structure 1133, 226-235.

[38] Huheey, J.E. (1965). The Electronegativity of Groups, J. Phys. Chem. 69, 3284-3291.

[39] S.G. Bratsch, (1985). A group electronegativity method with Pauling units, J. Chem. Edu. 62, 101-103.

[40] Keresztury, G.; Holly, S.; Besenyei, G.; Varga, J.; Wang, A.Y.; Durig, J.R. (1993). Vibrational spectra of monothiocarbamates-II. IR and Raman spectra, vibrational assignment, conformational analysis and ab initio calculations of S-methyl-N,N-dimethylthiocarbamate Spectrochim. Acta, 49A, 2007-2026.

[41] Michalska, D.; Wysokinski, R. (2005). The prediction of Raman spectra of platinum(II) anticancer drugs by density functional theory, Chemical Physics Letters, 403, 211-217.

[42] Chain, F.E.; Ladetto, M.F.; Grau, A.; Catalán, C.A.N.; Brandán, S.A. (2016). Structural, electronic, topological and vibrational properties of a series of N-benzylamides derived from Maca (Lepidium meyenii) combining spectroscopic studies with ONION calculations, J. Mol. Struct. 1105, 403-414.